Eur. Phys. J. E (2014) **37**: 78
DOI 10.1140/epje/i2014-14078-1

THE EUROPEAN PHYSICAL JOURNAL E

Regular Article

Segregation of chain ends to the surface of a polymer melt

M.W. Matsen[1,2,a] and P. Mahmoudi[1]

[1] Department of Chemical Engineering, University of Waterloo, Waterloo, Ontario, Canada
[2] Department of Physics & Astronomy, University of Waterloo, Waterloo, Ontario, Canada

Received 18 June 2014 and Received in final form 12 July 2014
Published online: 28 August 2014 –

Abstract. Self-consistent field theory (SCFT) is used to examine the surface of an incompressible polymer melt of freely jointed chains, each consisting of N discrete monomers connected by bonds of an arbitrary potential. As a result of entropic considerations, the end monomers tend to accumulate in a narrow region next to the surface (on the monomer scale), which causes a slight depletion of ends further into the melt (on the molecular scale). Due to the reduced configurational entropy available to polymers in the vicinity of a surface, we find an entropic contribution to the surface tension that increases with the degree of polymerization, N. While many quantities are dependent on the precise bond potential connecting the monomers, the excess of ends at the surface in the limit of infinite N, the functional form of the long-range depletion of ends, and the N dependence of the surface tension turn out to be universal.

1 Introduction

Nothing is boundless, and consequently surfaces are an important consideration in materials science. Usually surface effects are localized to the atomic scale, but the depth of these effects can potentially extend much further into the material for polymeric systems on account of the large molecular dimensions. In a polymer melt, for example, the chains obey random-walk statistics but the presence of a surface eliminates some of the configurations, reducing the entropy of all the polymers within reach of the surface. To a good approximation though, the surface simply reflects the random walks, leaving the polymer statistics relatively unaffected [1]. For instance, the concentration distribution of any specific monomer of the chain (*e.g.*, an end) remains uniform up to the edge of the surface. There is still, however, a reduction in entropy that contributes to the surface tension, but it is independent of the size of the polymers. An interesting consequence is that there is no effective interaction between solid objects immersed in a polymer melt until their separation becomes comparable to the Kuhn length of the polymer.

Experimental measurements [2–4] of the surface tension do, nevertheless, observe a dependence on molecular weight. One explanation is that, for real polymers, the end monomers have slightly different interactions with the surface than middle monomers [5,6]. Depending on the details of the interactions, this will result in either a depletion or excess of ends at the surface. Since the number of ends in the melt is inversely proportional to the size or polymerization, N, of the polymers, the segregation causes a N^{-1} correction to the surface tension. Evidently though, there is also an entropic contribution to the effect. An excess of chain ends occurs even in simulations [7–12], where end monomers are treated identically to middle monomers.

Indeed, Wu *et al.* [13] have since discovered an entropic explanation for the experiments. They performed a self-consistent field calculation for a compressible melt of Gaussian chains, where deviations from bulk concentration were penalized by a simple harmonic potential, resulting in a polymer surface of finite width, ξ. Their calculation predicted an excess of chain ends near the surface followed by a compensating depletion on the molecular length scale, and the resulting surface tension exhibited a N^{-1} correction for chains of finite size. As the authors pointed out, the slight depletion should also create a long-range interaction between solid objects. These effects, however, rely crucially on the compressibility of the polymer melt, and they, in fact, vanish in the incompressible limit where $\xi \to 0$.

Here we examine a completely different entropic mechanism for the segregation of ends to the surface, which also produces a N^{-1} correction to the surface tension. In this case, the effect results from the discreteness of the polymer chain, rather than the finite compressibility of the polymer melt. Thus we are able to study it on its own by simply considering an incompressible melt, where the polymer melt exhibits a sharp step profile that jumps from zero concentration immediately to a uniform bulk concentration. However, to see the effect, we need to replace the continuous Gaussian chain model that treats the polymers

[a] e-mail: mwmatsen@uwaterloo.ca

as thin elastic threads with one that retains the individual monomers. Apart from these two changes, our calculation proceeds in much the same way as the one by Wu *et al.*

2 SCFT for discrete chains

This section describes the self-consistent field theory (SCFT) for a melt of n discrete polymers, each consisting of N monomers connected by freely jointed bonds of potential energy, $u_b(\mathbf{R})$, where $\mathbf{R}$ denotes the bond vector. The theory is applied to an incompressible melt with a bulk monomer concentration of ρ_0 in contact with a flat wall. As usual in SCFT, the molecular interactions controlling the polymer concentration are replaced by an effective field, $w(\mathbf{r})$, which allows us to define a single-chain Hamiltonian

$$H[\{\mathbf{r}_i\}] = \sum_{i=1}^{N-1} u_b(\mathbf{r}_{i+1} - \mathbf{r}_i) + \sum_{i=1}^{N} w(\mathbf{r}_i), \tag{1}$$

where $\{\mathbf{r}_i\}$ specifies the positions of its N monomers. That simplification, in turn, allows us to perform the statistical mechanics exactly [14], whereby a dimensionless concentration of the i-th monomer,

$$\phi_i(\mathbf{r}) = \frac{V}{\mathcal{Q}} \frac{G_i(\mathbf{r}) G_{N+1-i}(\mathbf{r})}{h(\mathbf{r})}, \tag{2}$$

is expressed in terms of a propagator, $G_i(z)$, a Boltzmann weight for the field acting on a single monomer, $h(\mathbf{r}) \equiv \exp(-w(\mathbf{r})/k_BT)$, the volume of the melt, $V = nN/\rho_0$, and a single-chain partition function,

$$\mathcal{Q} = \int \frac{G_i(\mathbf{r}) G_{N+1-i}(\mathbf{r})}{h(\mathbf{r})} \mathrm{d}\mathbf{r}. \tag{3}$$

The propagator is evaluated by applying the recursive equation

$$G_{i+1}(\mathbf{r}) = h(\mathbf{r}) \int g(\mathbf{R}) G_i(\mathbf{r} - \mathbf{R}) \mathrm{d}\mathbf{R}, \tag{4}$$

starting from $G_1(\mathbf{r}) = h(\mathbf{r})$. Each iteration is a convolution with the Boltzmann weight, $g(\mathbf{R}) \propto \exp(-u_b(\mathbf{R})/k_BT)$, of the bond potential. For convenience, we normalize the weight such that

$$\int g(\mathbf{R}) \mathrm{d}\mathbf{R} = 1, \tag{5}$$

so that the statistical length of an unperturbed bond is given by

$$a = \left[\int R^2 g(\mathbf{R}) \mathrm{d}\mathbf{R} \right]^{1/2}. \tag{6}$$

In the bulk, the polymer chains obey random-walk statistics with an average end-to-end length of $a(N-1)^{1/2}$. This is generally well approximated by $aN^{1/2}$, which serves as a convenient measure for the typical molecular size of the polymers.

We position the wall with its surface at $z = 0$, so that $w(z)$, $h(z)$, $G_N(z)$ and $\phi_i(z)$ possess translational invariance in the x and y directions. This invariance allows us to complete the integration over X and Y in eq. (4), which in effect transforms $g(\mathbf{R})$ into

$$g(Z) \equiv \int g(\mathbf{R}) \mathrm{d}X \, \mathrm{d}Y. \tag{7}$$

In this way, the vectors, $\mathbf{r}$ and $\mathbf{R}$, in eq. (4) are converted into scalars, z and Z, reducing the recursion relation to a simple one-dimensional integral. Furthermore, $h(z) = 0$ in the region occupied by the wall, and thus $G_i(z) = 0$ for $z < 0$, which means that the integration only needs to be performed for $Z \leq z$.

For an incompressible melt, the field, $w(z)$, has to be adjusted so that the total polymer concentration,

$$\phi(z) = \frac{1}{N} \sum_{i=1}^{N} \phi_i(z), \tag{8}$$

is uniformly equal to one. This is achieved iteratively by simple mixing, where the $(m+1)$-th iteration of the field is given by

$$\frac{w^{(m+1)}(z)}{k_BT} = \frac{w^{(m)}(z)}{k_BT} + \lambda(\phi(z) - 1). \tag{9}$$

The mixing parameter, λ, is typically fixed at a value between 0.01 and 0.1, and the iteration is started from either $w^{(0)}(z) = 0$ or a previous solution obtained for similar parameter values. The iteration is repeated until

$$\frac{1}{L} \left[\int_0^L (\phi(z) - 1)^2 \mathrm{d}z \right]^{1/2} < \varepsilon, \tag{10}$$

where L is the system size in the z direction. We generally choose $L = 6aN^{1/2}$ and $\varepsilon = 10^{-6}$, which provides more than sufficient numerical accuracy. Once the field is known, the free energy, F, of the melt can be evaluated using

$$\frac{F}{nk_BT} = -\ln\left(\frac{\mathcal{Q}}{V}\right) - \frac{N}{k_BTL} \int_0^L w(z)\phi(z) \mathrm{d}z. \tag{11}$$

As must be the case, the concentration profiles and the free energy are unaffected by additive constants to the field, and so for convenience we shift the field so that $w(z) \to 0$ as $z \to \infty$. With this choice, $G_i(z) \to 1$ and consequently the self-consistent solution must satisfy $\mathcal{Q} = V$ in order that $\phi(z) \to 1$ in the bulk region. Hence the concentration of the end monomers becomes

$$\phi_e(z) \equiv \phi_1(z) = G_N(z). \tag{12}$$

Furthermore, the excess free energy per unit area or surface tension reduces to

$$\gamma_{\mathrm{en}} = -\rho_0 \int w(z) \mathrm{d}z. \tag{13}$$

Because our calculation creates the surface by constraining the polymer concentration rather than with molecular interactions, the surface tension only includes the polymeric part due to chain connectivity. One can more or less regard $\gamma_{\rm en}$ as the entropic contribution to the surface tension, which adds to the enthalpic contribution that exists for a simple liquid of unreacted monomers (*i.e.*, $N = 1$)[1].

3 Results

We begin by considering monomers bonded by Hookean springs, for which the Boltzmann weight of the bond potential is

$$g(\mathbf{R}) = \left(\frac{3}{2\pi a^2}\right)^{3/2} \exp\left(-\frac{3R^2}{2a^2}\right), \tag{14}$$

and the integrated Boltzmann weight is

$$g(Z) = \left(\frac{3}{2\pi a^2}\right)^{1/2} \exp\left(-\frac{3Z^2}{2a^2}\right). \tag{15}$$

The segregation of ends to the surface is shown in fig. 1(a) for chains with different degrees of polymerization, N, while the self-consistent field required to satisfy incompressibility is plotted in fig. 1(b). Starting with no segregation for $N = 1$, an excess of end monomers emerges at the surface, increasing monotonically as the chains become longer and eventually reaching the asymptote denoted by the red curve. Naturally this excess, which occurs over the monomer length scale (*i.e.*, $0 \le z \lesssim a$), has to be balanced by a depletion elsewhere. As we will see in sects. 3.2 and 3.3, there is a shallow depletion immediately following the excess that extends over the molecular length scale (*i.e.*, $a \lesssim z \lesssim aN^{1/2}$).

In order to help distinguish between universal and model-dependent features, we repeat the calculations for a second model consisting of rigid bonds of fixed length, where

$$g(\mathbf{R}) = \frac{1}{4\pi a^2}\delta(R - a), \tag{16}$$

and

$$g(Z) = \begin{cases} (2a)^{-1}, & \text{if} \quad |Z| \le a, \\ 0, & \text{if} \quad |Z| > a. \end{cases} \tag{17}$$

Figure 2 shows the analogous results for this alternative model. Interestingly, the self-consistent field has precisely the same value at the wall

$$\frac{w(0)}{k_BT} = -1 + \frac{1}{N}. \tag{18}$$

This follows from an identity derived previously (eq. (32) in ref. [14]). The level of end-monomer segregation at the surface, $\phi_e(0)$, is nearly the same for both chain models, but there is a small difference for finite values of N. Surprisingly however, they do become identical in the $N \to \infty$ limit, as we will demonstrate shortly in sect. 3.1.

[1] This division is not exact since $\gamma_{\rm en}$ does include the internal energy of the bonds, and furthermore the polymer profile and thus the entropy would change slightly if we used molecular interactions to form the polymer surface.

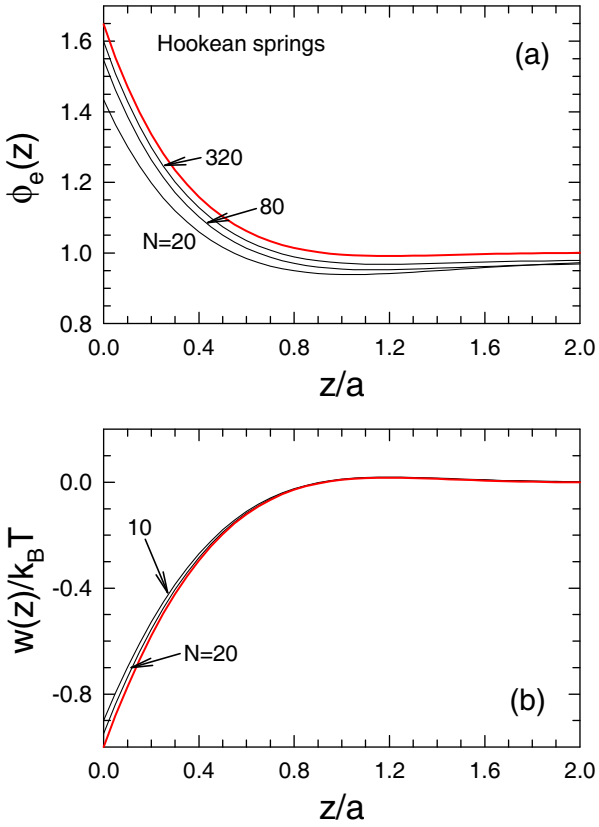

Fig. 1. (a) End-monomer distribution and (b) self-consistent field for polymer chains each consisting of N monomers connected by Hookean springs. The red curves denote the $N \to \infty$ limit.

3.1 Infinite chain limit

The first step in our analysis of the results is to evaluate the $N \to \infty$ limit, denoted by the red curves in figs. 1 and 2. This is again done iteratively, usually starting with a self-consistent solution for a large but finite N, which serves as a good initial guess for $G_\infty(z)$ and $h_\infty(z) \equiv \exp(-w_\infty(z)/k_BT)$. Each iteration is performed by applying the recursion relation in eq. (4) a couple thousand times to improve our estimate of $G_\infty(z)$. Next we refine our estimate of $w_\infty(z)$ by applying the same simple mixing step described earlier, but with the large-N approximation,

$$\phi(z) = \frac{V}{\mathcal{Q}} \frac{G_\infty^2(z)}{h_\infty(z)}, \tag{19}$$

for the polymer concentration and

$$\mathcal{Q} = \int \frac{G_\infty^2(z)}{h_\infty(z)} \, \mathrm{d}\mathbf{r}, \tag{20}$$

for the single-chain partition function. This process is repeated until $\phi(z) = 1$ to within our usual error tolerance. When we are done, the resulting propagator satisfies

$$G_\infty(z) = h_\infty(z) \int g(Z) G_\infty(z - Z) \mathrm{d}Z, \tag{21}$$

$$= \sqrt{h_\infty(z)}. \tag{22}$$

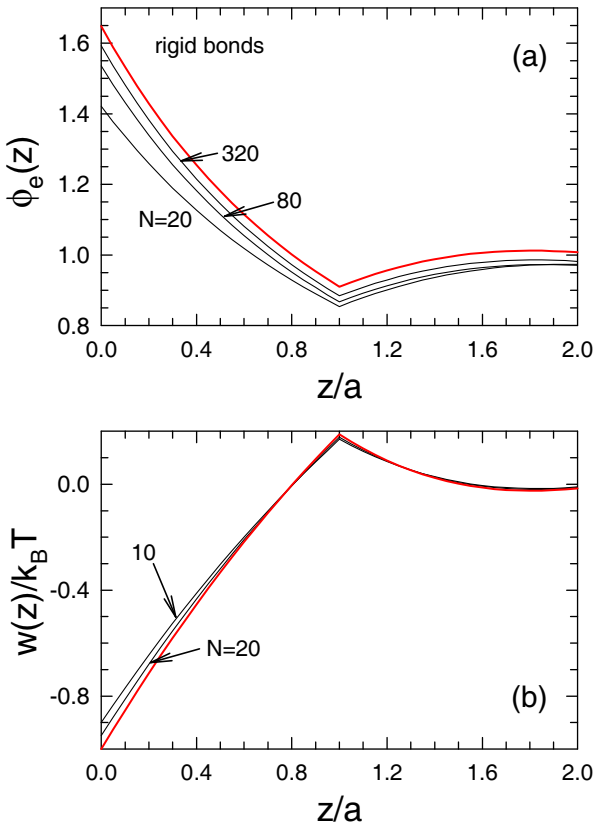

Fig. 2. Analogous plots to those in fig. 1, but calculated for chains with rigid bonds of fixed length, a.

As clearly evident from comparing figs. 1(a) and 2(a), the short-range excess of chain ends, $\phi_e(z) \approx G_\infty(z)$, depends on the details of the model. However, the excess at the wall approaches a universal value in the $N \to \infty$ limit. The asymptote is obtained by combining eq. (22) with eq. (18) to give

$$G_\infty(0) = \sqrt{e} = 1.6487\ldots, \tag{23}$$

which indeed matches the red curves in figs. 1(a) and 2(a).

3.2 Finite chains in $w_\infty(z)$

As mentioned previously, the short-range excess is balanced by a small dip in concentration extending over the molecular length scale. To work this out, we start by considering finite chains in the self-consistent field of infinitely long ones. Figure 3(a) shows the resulting propagator, $G_N^0(z)$, for polymers of different polymerization in the field $w_\infty(z)$. From previous works [14,15], we can anticipate the approximation

$$G_N^0(z) \approx G_\infty(z) + A\sqrt{\frac{6}{\pi N}} \times \left[\exp\left(-\frac{3z^2}{2a^2N}\right) + G_\infty(z) - 1\right], \tag{24}$$

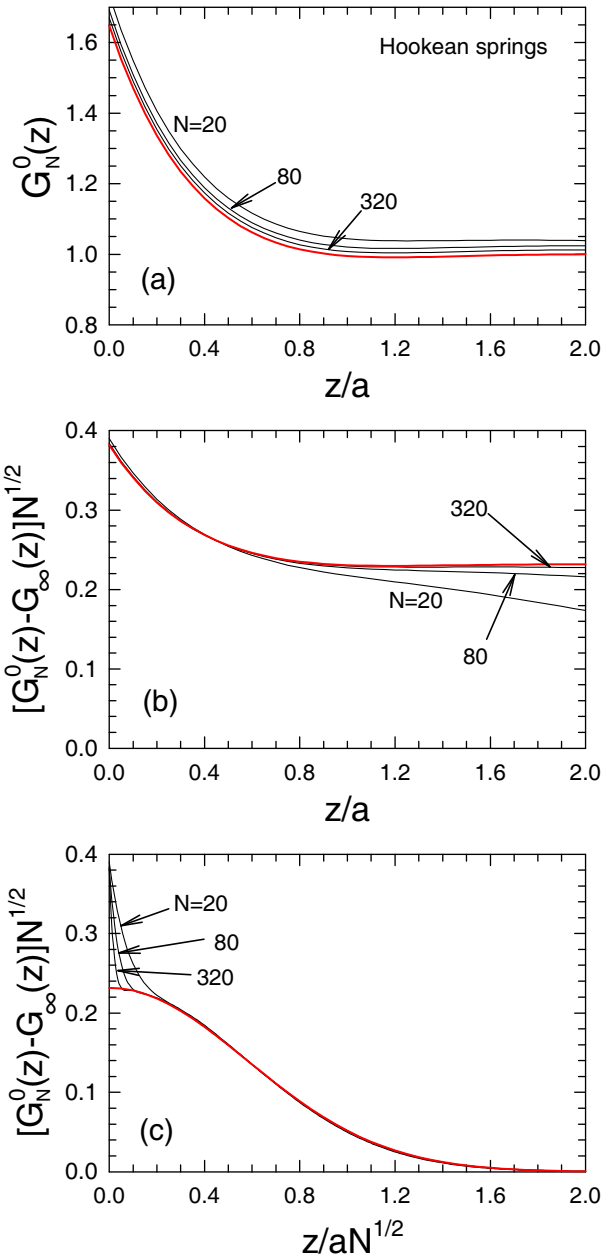

Fig. 3. (a) Propagator, $G_N^0(z)$, for finite chains in the self-consistent field, $w_\infty(z)$, of infinite polymers. The extra concentration of end monomers relative to $G_\infty(z)$ is plotted on the (b) monomer scale and (c) molecular scale. The red curves denote the $N \to \infty$ limit, as implied by eq. (24).

where the $N^{-1/2}$ correction involves a long-range Gaussian with a short-range part that maintains the proportionality $G_N^0(z) \propto G_\infty(z)$ for $z \lesssim a$. Figures 3(b) and 3(c) confirm the short- and long-range parts of the correction, respectively.

Figure 4 shows the polymer concentration, $\phi^0(z)$, of finite chains in the self-consistent field for infinite polymers, normalized so that $\phi^0(z) \to 1$ in the bulk (*i.e.*, using eq. (2) with $\mathcal{Q} = V$). This can be estimated by inserting the approximation for the propagator from eq. (24) into

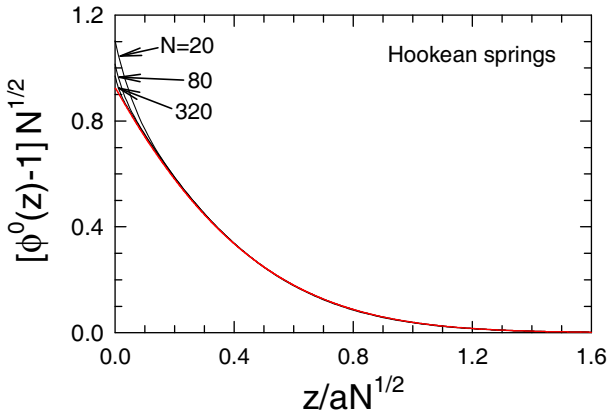

Fig. 4. Excess polymer concentration near the surface for finite chains in the self-consistent field of infinite chains. The red curve denotes the large-N estimate in eq. (25).

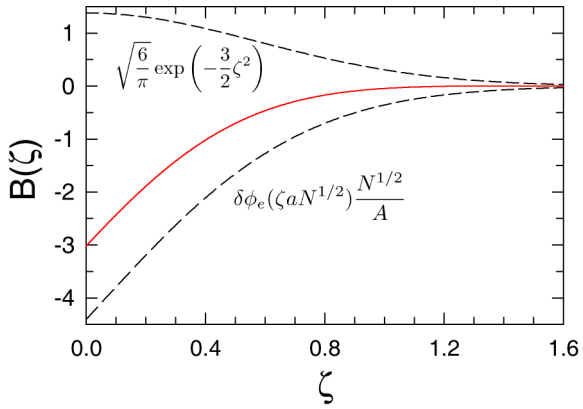

Fig. 5. Universal shape of the long-range depletion of chain ends that balances the short-range excess. The dashed curves show the contributions from $G_N^0(z)$ in eq. (24) and $\delta\phi_e(z)$ corresponding to eq. (33).

eq. (2), and approximating the sum in eq. (8) by an integral. Keeping terms to order $N^{-1/2}$, we obtain

$$\phi^0(z) \approx 1 + 2A\sqrt{\frac{6}{\pi N}} \int_0^1 \frac{1}{\sqrt{s}} \exp\left(-\frac{3z^2}{2a^2Ns}\right) \mathrm{d}s, \quad (25)$$

which is plotted in fig. 4 with a red curve.

The constant, A, in eq. (25) is determined by examining the excess concentration of monomers to zeroth order in N. The excess of ends, which is given by the integral of $G_N^0(z) - 1$ from eq. (24), has a short-range contribution equal to the integral of $G_\infty(z) - 1$, and a long-range contribution of Aa. On the other hand, the excess of middle monomers, which is the integral of $\phi^0(z) - 1$, just has a long-range contribution of $2Aa$. The connectivity of the chains requires these excesses to balance, which implies that Aa equals the short-range excess of end monomers. For the two models considered here, numerical integration gives

$$A = \frac{1}{a}\int_0^\infty [G_\infty(z) - 1]\mathrm{d}z, \quad (26)$$

$$= \begin{cases} 0.167743 & \text{for Hookean springs,} \\ 0.198234 & \text{for rigid bonds,} \end{cases} \quad (27)$$

for the short-range excess of end monomers.

3.3 Perturbation to $w_\infty(z)$

For finite polymer chains, the field needs to be adjusted to remove the excess polymer concentration, $\phi_0(z) - 1$, plotted in fig. 4. Since the excess is small in amplitude and long range in extent, we correct $w_\infty(z)$ by using the linear response theory for continuous Gaussian chains [13]. In Fourier space, the change in concentration, $\delta\phi(z)$, predicted by linear response theory is related to the change in field, $\delta w(z)$, by

$$\delta\phi(k) = -\frac{Ns_\phi(x)}{k_BT}\delta w(k), \quad (28)$$

where

$$s_\phi(x) = \frac{2(e^{-x} + x - 1)}{x^2} \quad (29)$$

is the Debye function and $x = k^2a^2N/6$. Similarly, the linear response for the ends is given by

$$\delta\phi_e(k) = -\frac{Ns_e(x)}{k_BT}\delta w(k), \quad (30)$$

where

$$s_e(x) = \frac{1 - e^{-x}}{x} \quad (31)$$

is a Debye-like function for the ends.

From eq. (25), it follows that the Fourier transform[2] of the required change in concentration, $\delta\phi(z) = 1 - \phi^0(z)$, is

$$\delta\phi(k) = -Aa\sqrt{\frac{8}{\pi}}s_e(x). \quad (32)$$

Combining this with eqs. (28) and (30), we obtain the corresponding change in the end-monomer concentration,

$$\delta\phi_e(k) = -Aa\sqrt{\frac{8}{\pi}}\frac{s_e^2(x)}{s_\phi(x)}. \quad (33)$$

This is converted back to real space, $\delta\phi_e(z)$, by performing the inverse Fourier transform numerically. The result is plotted in fig. 5 and added to the Gaussian contribution from eq. (24) to give a universal shape for the long-range depletion of end monomers, $B(z/aN^{1/2})$. The fact that $\delta\phi(k) = \delta\phi_e(k)$ at $k = 0$ implies that

$$\int_0^\infty B(\zeta)\mathrm{d}\zeta = -1, \quad (34)$$

which ensures that the long-range depletion balances the short-range excess in eq. (26).

[2] Technically, our spatial functions are only defined for $z \geq 0$, and therefore we Fourier transform the even functions obtained by reflecting about $z = 0$.

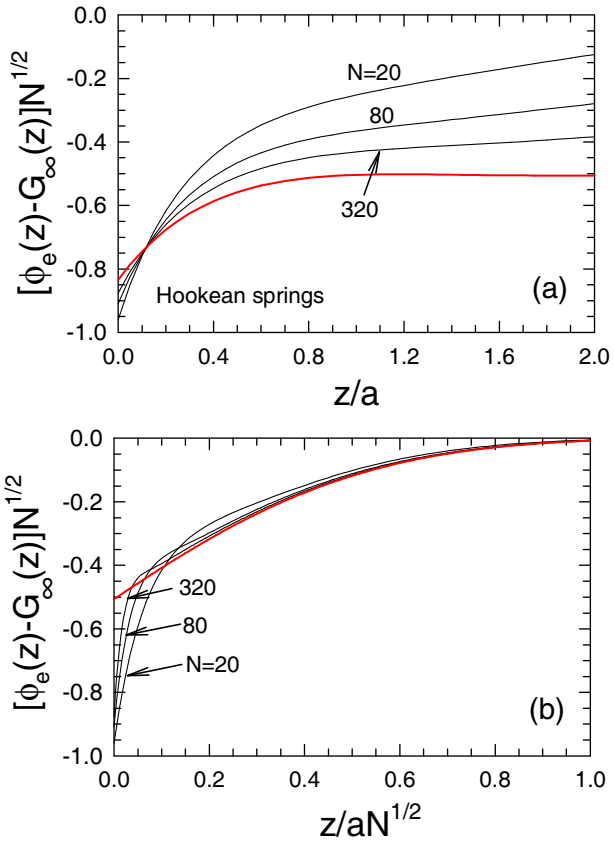

Fig. 6. Deviations from $\phi_e(z) \approx G_\infty(z)$ on the (a) monomer and (b) molecular length scales for chains each consisting of N monomers connected by Hookean springs. The red curves show the large-N limits from eq. (35), $AB(0)[G_\infty(z)-1]$ and $AB(z/aN^{1/2})$, respectively.

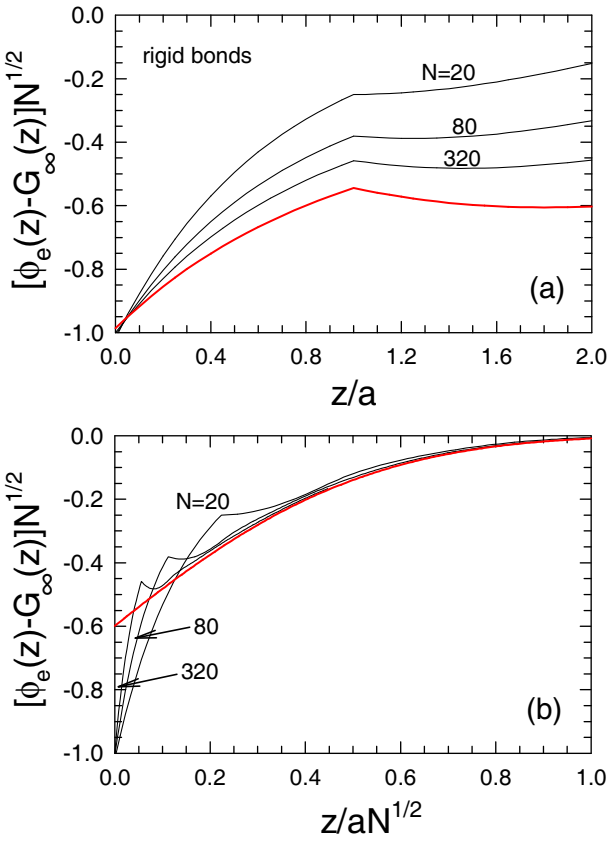

Fig. 7. Analogous plots to those in fig. 6, but calculated for chains with rigid bonds of fixed length, a.

Now that the field has been corrected to remove the excess polymer concentration in fig. 4, the end-monomer distribution takes the form

$$\phi_e(z) \approx G_\infty(z) + \frac{A}{N^{1/2}} \left\{ B\left(\frac{z}{aN^{1/2}}\right) + B(0)[G_\infty(z)-1] \right\}. \tag{35}$$

As before, a factor of $G_\infty(z)-1$ is added to eq. (35), so that $\phi_e(z) \propto G_\infty(z)$ in the vicinity of the wall. Figures 6(a) and 6(b) confirm the short- and long-range parts of the $N^{-1/2}$ correction, respectively, for the Hookean spring model. Likewise, analogous plots in fig. 7 demonstrate the validity of the corrections for chains with rigid bonds of fixed length.

3.4 Surface tension

Lastly, we evaluate the entropic contribution to the surface tension, $\gamma_{\rm en}$, using the expression derived in eq. (13). It is plotted in fig. 8 for polymer chains with Hookean springs (circles) as well as with rigid bonds (diamonds). In both cases, the entropic surface tension starts from zero for monomers (*i.e.*, $N = 1$) and reaches an asymptote limit for infinite chains (*i.e.*, $\gamma_{\rm en}/a\rho_0 k_B T \to \Gamma_\infty$ for $N \to \infty$),

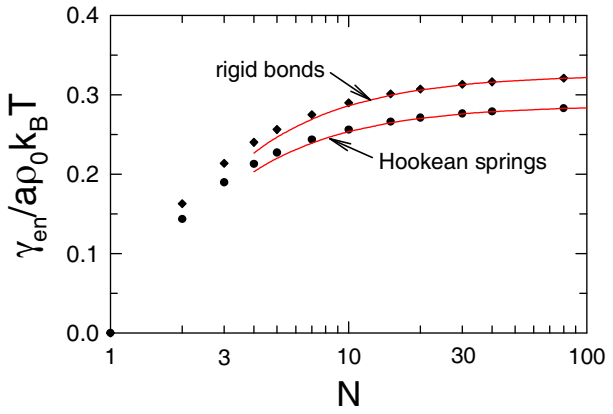

Fig. 8. Entropic contribution to the surface tension due to chain connectivity for polymers consisting of N monomers joined by Hookean springs (circles) and by rigid bonds (diamonds). The curves denote the approximation in eq. (40).

where

$$\Gamma_\infty = \frac{1}{ak_BT} \int_0^\infty w_\infty(z) \mathrm{d}z, \tag{36}$$

$$= \frac{2}{a} \int_0^\infty \ln G_\infty(z) \mathrm{d}z, \tag{37}$$

$$= \begin{cases} 0.28712 & \text{for Hookean springs,} \\ 0.32587 & \text{for rigid bonds.} \end{cases} \tag{38}$$

To obtain an estimate for finite chains, we just need to account for the change in the field, $\delta w(z)$, calculated by the linear response theory. Using the fact that $s_\phi(0) = 1$, eq. (28) implies that

$$\int_0^\infty \delta w(z)\mathrm{d}z = -\frac{k_BT}{N}\int_0^\infty \delta\phi(z)\mathrm{d}z = \frac{2Aak_BT}{N}\,. \quad (39)$$

Although we are applying the linear response theory for continuous Gaussian chains, this identity also holds for discrete chains. Using eq. (39), it then follows that

$$\frac{\gamma_{\mathrm{en}}}{a\rho_0 k_BT} \approx \Gamma_\infty - \frac{2A}{N}\,. \quad (40)$$

Incredibly, this expression remains accurate for polymer chains as short as four monomers, as illustrated by the red curves in fig. 8.

4 Discussion

Although we have described our system as a polymer melt in contact with a hard wall, our calculation applies to any surface with a sufficiently sharp polymer profile. By assuming an incompressible melt, we were able to ignore the interactions responsible for creating the surface, whether they be those of a wall or just the cohesive attraction between monomers. This is because the combined energy of the interactions remains constant on account of the fixed polymer concentration, and thus they do not affect the polymer statistics. Of course, the interactions responsible for forming the surface would contribute to the enthalpic part of the surface tension, but the entropic part plotted in fig. 8 should remain relatively unaffected. This simplification, however, overlooks the layering of monomers that generally occurs next to an atomically flat wall [7,9,16], causing damped oscillations in the average polymer concentration. Thus our calculation may be somewhat more appropriate to a high-tension air/polymer surface, where the concentration increases smoothly from zero to the bulk value over a narrow width on the order of the monomer size (*i.e.*, $\xi \sim a$) [16]. Even still, the mean-field theory will neglect the correlations between monomers due to their excluded volume; see refs. [17,18] for a discussion of these effects. While the correlations will modify somewhat the short-range part of the end-monomer distribution, $G_\infty(z)$, they should have relatively little effect on the long-range part, $B(z/aN^{1/2})$.

Our results can readily be compared to simulations by Bitsanis and Hadziioannou [8] and by Kumar *et al.* [9]. Both simulations examined melts of freely jointed chains, where monomers interacted via a truncated Lennard-Jones potential and bonded monomers were connected by FENE springs. The former simulations examined relatively short chains ($5 \le N \le 30$) at modest densities, while the later ones considered longer chains ($50 \le N \le 200$) at relatively high densities. The bonds in this model tend to be rather stiff and thus correspond best to our calculation for rigid bonds. Consistent with our calculation, both simulations found a surface enhancement of end monomers that increased with molecular weight. Those of Bitsanis and Hadziioannou observed end monomer concentrations of up to 1.7 times that of the bulk, which is somewhat higher than our asymptotic limit in eq. (23). On the other hand, Kumar *et al.* only saw enhancements of up to 1.4, which is somewhat lower than our predictions. Note, however, that the simulations calculate average concentrations over finite intervals (or bins), which will reduce the concentration measured at the wall. Thus the simulations by Kumar *et al.* appear to be in better agreement with our predictions, perhaps because they were performed at higher polymer concentration.

Our SCFT calculation is very similar in nature to the one of Wu *et al.* [13], as are our results. Their calculations also predicted a short-range excess of ends followed by a long-range depletion, and furthermore they predicted a N^{-1} correction to the surface tension for chains of finite length. However, their model is significantly different and the mechanism for the surface segregation of ends has an altogether different origin. Unlike our calculation where the polymer concentration immediately drops to zero at the wall, the calculation by Wu *et al.* included a finite compressibility such that the concentration decayed to zero over a finite width, ξ. The effect they observed is intimately related to this finite compressibility. Indeed, the surface segregation of ends vanishes and the surface tension diverges in the limit of zero compressibility (*i.e.*, $\xi \to 0$), whereas in our calculation both quantities remain finite despite the incompressibility.

At first glance, the fact that we obtain finite results for an incompressible melt may seem to contradict the calculation by Wu *et al.* [13]. The essential difference is that we use a discrete model, whereas Wu *et al.* employ the continuous Gaussian chain model that treats the polymers as thin elastic threads. The later is a coarse-grained model, where N, a and ρ_0 refer to segments each consisting of many monomers. We can coarse grain our model by defining segments involving m monomers, which is simply done by making the substitutions: $N \to Nm$, $a \to am^{-1/2}$ and $\rho_0 \to \rho_0 m$. With that the surface tension in eq. (13) becomes

$$\frac{\gamma_{\mathrm{en}}}{a\rho_0 k_BT} = \Gamma_\infty m^{1/2} - \frac{2A}{N}m^{-1/2}, \quad (41)$$

which diverges as $m \to \infty$. Furthermore, the coarse graining washes out the end-monomer enrichment at the surface, because the end segment is now an average concentration over the last m monomers of the chain. Hence, our results are consistent with those of Wu *et al.*

An implicit assumption in the SCFT calculation of Wu *et al.* [13] is that the width of the polymer profile remains large relative to the size of a course-grained segment (*i.e.*, $\xi \gg a$). This may be a reasonable assumption for polymer/polymer or polymer/solvent interfaces, but it does really not hold for sharp polymer/wall or polymer/air surfaces. Müller *et al.* [12] recognized this problem when comparing their simulations of discrete chains to the SCFT predictions for compressible Gaussian chains, which lead them to propose a correction to the SCFT. In any case, the effect predicted by Wu *et al.* should still be qualitative present for narrow surfaces. Therefore, it would be

interesting to generalize our calculation to include finite compressibility and thus examine both surface segregation effects together. Although this will certainly alter the details of the short-range excess, the shape of the long-range depletion plotted in fig. 5 should still remain the same.

5 Summary

Our study examined the distribution of chain ends, $\phi_e(z)$, near the surface of an incompressible polymer melt using self-consistent field theory (SCFT). Rather than using the usual Gaussian chain model, we applied the SCFT to discrete chains consisting of N monomers joined by flexible bonds of arbitrary potential, $u_b(R)$. The method was demonstrated for two different models, one with Hookean springs (*i.e.*, $u_b(R) \propto R^2$) and another with rigid bonds (*i.e.*, $u_b(R) \propto \delta(R-a)$).

For large N, $\phi_e(z) \approx G_\infty(z)$, where $G_\infty(z)$ is a fixed point of the recursion relation, eq. (4), for the polymer propagator. Interestingly, the fixed point has a universal (*i.e.*, model-independent) value of $G_\infty(0) = \sqrt{e}$ at the wall, corresponding to a 65% enrichment of ends. The shape of $G_\infty(z)$, however, is model dependent but in all cases is short ranged (*i.e.*, $G_\infty(z) \to 1$ for $z \gg a$). The enrichment is compensated for by a long-range depletion that has a universal shape, $B(z/aN^{1/2})$, with an amplitude of $AN^{-1/2}$, where A is the integrated short-range excess divided by the bond length, eq. (26). The configurational entropy lost by polymers in the vicinity of the surface creates an entropic contribution to the surface tension, γ_{en}, that is extremely well approximated by an asymptotic value, Γ_∞, and a finite-N correction proportional to A/N. Note that our calculation omits the enthaplic part of the surface tension, because it creates the surface by applying a constraint rather than by including molecular interactions; however, the enthalpic contribution should be relatively independent of N.

The mechanism of chain end segregation studied here is distinct from the one examined previously by Wu *et al.* [13], which relies on a finite compressibility of the polymer melt and a finite width to the surface profile. Our effect, on the other hand, relies on the discreteness of the polymer chain. An obvious next step would be to generalize our calculation by including compressibility, so as to account for both mechanisms simultaneously.

We are grateful to Jamie Forrest and Dave Morse for useful discussions. This work was supported by startup funds from the University of Waterloo.

References

1. A. Silberberg, J. Colloid Interface Sci. **90**, 86 (1982).
2. C. Jalbert, J.T. Koberstein, I. Yilgor, P. Gallagher, V. Krukonis, Macromolecules **26**, 3069 (1993).
3. S.H. Anastasiadis, I. Gancarz, J.T. Koberstein, Macromolecules **21**, 2980 (1988).
4. B.B. Sauer, G.T. Dee, J. Colloid Interface Sci. **162**, 25 (1994).
5. P.G. de Gennes, C.R. Acad. Sci. Paris **307**, 1841 (1988).
6. J.H. Jang, R. Ozisik, W.L. Mattice, Macromolecules **33**, 7663 (2000).
7. S.K. Kumar, M. Vacatello, D.Y. Yoon, J. Chem. Phys. **89**, 5206 (1988).
8. I. Bitsanis, G. Hadziioannou, J. Chem. Phys. **92**, 3827 (1990).
9. S.K. Kumar, M. Vacatello, D.Y. Yoon, Macromolecules **23**, 2189 (1990).
10. A. Yethiraj, C.K. Hall, Macromolecules **23**, 1865 (1990).
11. R.S. Pai-Panandike, J.R. Dorgan, T. Pakula, Macromolecules **30**, 6348 (1997).
12. M. Müller, B. Steinmüller, K.C. Daoulas, A Ramírez-Hernández, J.J. de Pablo, Phys. Chem. Chem. Phys. **13**, 10491 (2011).
13. D.T. Wu, G.H. Fredrickson, J.-P. Carton, A. Ajdari, L. Leiber, J. Polym. Sci., Part B: Polym. Phys. **33**, 2373 (1995).
14. M.W. Matsen, J.U. Kim, A.E. Likhtman, Eur. Phys. J. E **29**, 107 (2009).
15. I.Y. Erukhimovich, A. Johner, J.F. Joanny, Eur. Phys. J. E **27**, 435 (2008).
16. K.C. Daoulas, V.A. Harmandaris, V.G. Mavrantzas, Macromolecules **38**, 5780 (2005).
17. P. Virnau, K. Binder, H. Heinz, T. Kreer, M. Müller, in *Encyclopedia of Polymer Blends*, Vol. **1**: *Fundamentals*, edited by A.I. Isayev (Wiley-VCH, Weinheim, 2010).
18. J.P. Wittmer, A. Cavallo, H. Xu, J.E. Zabel, P. Poliüska, N. Schulmann, H. Meyer, J. Fatago, A. Johner, S.P. Obukhov, J. Baschnagel, J. Stat. Phys. **145**, 1017 (2011).